Petroleum Science (2018) 15:319–334
https://doi.org/10.1007/s12182-018-0218-1

ORIGINAL PAPER

Mudcake effects on wellbore stress and fracture initiation pressure and implications for wellbore strengthening

Yongcun Feng[1] · Xiaorong Li[1] · K. E. Gray[1]

Received: 5 September 2017 / Published online: 9 March 2018

Abstract
Although a large volume of mudcake filtration test data is available in the literature, effects of mudcake on wellbore strengthening cannot be quantified without incorporating the data into a stress-analysis model. Traditional models for determining fracture initiation pressure (FIP) either consider a wellbore with an impermeable mudcake or with no mudcake at all. An analytical model considering permeable mudcake is proposed in this paper. The model can predict pore pressure and stress profiles around the wellbore, and consequently the FIP, for different mudcake thickness, permeability, and strength. Numerical examples are provided to illustrate the effects of these mudcake parameters. The results show that a low-permeability mudcake enhances FIP, mainly through restricting fluid seepage and pore pressure increase in the near-wellbore region, rather than by mudcake strength. Fluid loss pressure (FLP) should be distinguished from FIP when a mudcake is present on the wellbore wall. Fracture may occur behind the mudcake at FIP without mudcake rupture. The small effect of mudcake strength on FIP does not mean its effect on FLP is small too. Mudcake strength may play an important role in maintaining integrity of the wellbore once a fracture has initiated behind the mudcake.

Keywords Mudcake · Hoop stress · Fracture initiation pressure · Fluid loss pressure · Wellbore strengthening

1 Introduction

As a bit drills through a permeable formation in overbalance drilling, the base fluid of drilling mud permeates into the formation while solid components are filtered out, leaving a mudcake on the wellbore wall. Both laboratory tests and field practices have shown that the presence of a mudcake can effectively inhibit fracture creation on the wellbore and thus prevent lost circulation (Cook et al. 2016; Guo et al. 2014; Song and Rojas 2006). Researchers also found that with some additives, such as lost circulation materials (LCMs), the drilling mud can improve the quality of the mudcake and better enhance wellbore strength (Ewy and Morton 2009; Song and Rojas 2006).

An optimal mudcake should have low permeability and thin thickness (Amanullah and Tan 2001). It is well known that fluid permeation through the wellbore wall increases the local pore pressure and decreases the effective hoop stress around the wellbore, resulting in a reduced fracture initiation pressure (FIP), i.e., the minimum wellbore pressure at which a fracture is created on the wellbore wall. Therefore, low permeability is required for the mudcake to prevent or mitigate base fluid permeation. On the other hand, although a thick mudcake can also help restrict fluid permeation, it may cause other drilling problems, such as stuck pipe and excessive torque and drag (Hashemzadeh and Hajidavalloo 2016; Ottesen et al. 1999; Outmans 1958). So a thick mudcake is usually not recommended.

The bottom hole conditions under which a mudcake forms are very complex. The development of the mudcake depends on a number of factors such as drilling mud constituents, wellbore pressure and temperature, pore pressure, formation permeability and porosity, annulus flow regime, and time (Hashemzadeh and Hajidavalloo 2016; Salehi and Kiran 2016). During dynamic drilling, the jets of the drilling bit may generate very turbulent flow and the rate of mudcake formation is controlled by two opposite actions—deposition and erosion (Cook et al. 2016; Mostafavi et al. 2010). Mudcake buildup stops when the deposition and erosion rates become equal. However, the

Edited by Yan-Hua Sun

✉ Yongcun Feng
yongcun.f@gmail.com

[1] The University of Texas at Austin, Austin, TX, USA

point at which the two rates equilibrate is difficult to determine. In this paper, it is assumed that the mudcake forms before the creation of any fracture.

Three important parameters dictating the effectiveness of mudcake on wellbore strengthening are mudcake thickness, permeability, and strength. Numerous researchers have experimentally investigated the development of these mudcake parameters under various borehole conditions. For example, Jaffal et al. (2017) and Griffith and Osisanya (1999) performed filtration tests and studied the effects of a number of factors (e.g., differential pressure, solids content, filtration control agent) on mudcake thickness and permeability. Yield strength of the mudcake has been extensively measured under different loading conditions (Bailey et al. 1998; Cerasi et al. 2001; Cook et al. 2016). Although a large volume of mudcake data is available in the literature, the effects of different mudcake parameters on wellbore strengthening cannot be quantified without incorporating the data into a stress-analysis model.

It is well known that a fracture initiates once the stress on the wellbore wall overcomes the concentrated hoop stress and the tensile strength of the rock (Chuanliang et al. 2015; Guo et al. 2017a, b; Zhu et al. 2014). Therefore, FIP (i.e., the wellbore pressure at the critical moment of fracture initiation) is determined by the hoop stress and the tensile strength. The tensile strength of rock is a measurable parameter. However, the hoop stress can be greatly altered by the formation of mudcake on the wellbore wall. Therefore, a model relating wellbore stress profile and mudcake properties is required for evaluating the effects of mudcake on FIP and optimizing mud design (Feng et al. 2018).

Traditional models for determining FIP assume two extreme conditions of the wellbore: a wellbore with an impermeable mudcake, e.g., the Hubbert–Willis model (Hubbert and Willis 1957), and a wellbore with no mudcake, e.g., the Haimson–Fairhurst model (Haimson and Fairhurst 1969). Obviously, these models cannot capture the effects of various parameters of a permeable mudcake on FIP, resulting in an overestimated FIP while assuming impermeable mudcake and underestimated FIP if the mudcake is not considered (Tran et al. 2011).

Therefore, an analytical model considering a permeable mudcake is proposed in this paper. The model is derived based on the assumptions of Darcy's fluid flow through the mudcake and formation and the superposition principle of elasticity. The model can be used to predict pore pressure and stress profiles around the wellbore, and consequently the FIP, for different mudcake thickness, permeability, and strength. Numerical examples are provided to illustrate the effects of these mudcake parameters.

It should be noted that FIP and fluid loss pressure (FLP—the critical wellbore pressure causing mud loss into the fracture) should be distinguished from each other. Because at the moment of fracture initiation on wellbore wall at FIP, the mudcake may remain unbroken and wellbore fluids cannot enter the fracture; thus, no fluid loss can be observed at FIP (Feng et al. 2016). Only when the mudcake eventually ruptures as the wellbore pressure increases, will significant fluid loss occur. However, from a conservative point of view, it is better to maintain wellbore pressure below FIP during drilling to avoid lost circulation. The difference between FIP and FLP is discussed in more detail in this paper.

2 Analytical mudcake model

In this section, an analytical mudcake model is derived, which takes into account the effects of mudcake thickness, permeability and strength on near-wellbore pore pressure and stress states, and thus FIP of the wellbore. A thin layer of mudcake is assumed on the inner surface of a wellbore subjected to non-uniform far-field stresses and pore pressure, as schematically depicted in Fig. 1. For deriving the model, the following assumptions are made:

- The wellbore, mudcake, and formation are in a plane-strain condition.
- The mudcake and wellbore rock bond perfectly. The inner mudcake radius, outer mudcake radius (i.e., wellbore radius), and outer formation radius are R_i, R_o, and R_e, respectively. The mudcake thickness is w ($w = R_o - R_i$).

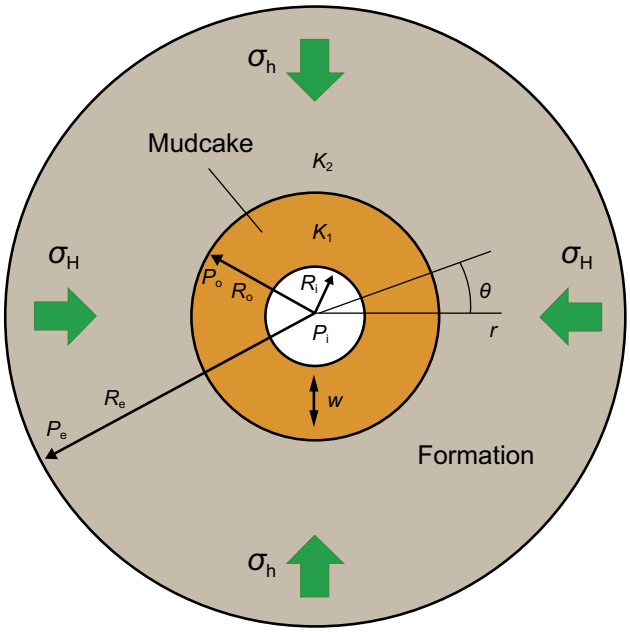

Fig. 1 Schematic of the cross section of wellbore, mudcake, and formation (not to scale)

- The permeabilities of the mudcake and formation are K_1 and K_2 ($K_2 > K_1$), respectively.
- Pore pressure at the outer formation boundary is not perturbed by the wellbore fluid and maintains constant at P_e. A constant mud pressure P_i ($P_i > P_e$) is applied on the inner surface of the mudcake.
- Fluid flow from the wellbore to the formation under the differential pressure is steady state and obeys Darcy's law.
- The formation rock is isotropic, homogeneous, and poroelastic material.
- The mudcake is very soft/flexible compared to the rock and has a very small yield strength so that it undergoes perfectly plastic yielding under wellbore pressure. Poisson's ratio for post-yield deformation of mudcake is assumed to be 0.5.
- Mudcake thickness and properties do not change with time.
- The maximum and minimum far-field total stresses are σ_H and σ_h, respectively.
- The sign convention for stress is compression as positive and tension as negative.

Pore pressure varies with radial distance in this problem due to fluid flow from the wellbore to the formation under differential pressure. The pore pressure distribution can be determined with Darcy's law. The total stress distribution around the wellbore is determined by four stress components induced by: (1) varying pore pressure around the wellbore, (2) far-field stresses, (3) wellbore pressure acting on the inner mudcake surface, and (4) the presence of mudcake. To simplify the problem, it is assumed that these terms are uncoupled and the final expression for total stress can be obtained by the superposition principal. The following subsections describe the detailed derivation processes for determining the total stress around the wellbore with the presence of a mudcake.

2.1 Total stresses around the wellbore induced by varying pore pressure

2.1.1 Varying pore pressure distribution around the wellbore

In order to determine the total stress induced by varying pore pressure, the pore pressure distribution around the wellbore should be determined first. Assuming the pore pressure at the wellbore wall (interface between mudcake and formation) is P_o, then according to Darcy's law for radial flow from the wellbore to the formation, one can obtain

$$\frac{2\pi K_1}{\mu_1 \ln\frac{R_o}{R_i}}(P_o - P_i) = \frac{2\pi K_2}{\mu_2 \ln\frac{R_e}{R_o}}(P_e - P_o) \tag{1}$$

where μ_1 and μ_2 are viscosities of fluids in the mudcake and rock, respectively. Assuming $\mu_1 = \mu_2$, the pore pressure at the wellbore wall can be obtain by rearranging Eq. (1) as

$$P_o = P_i - B\Delta P_o \tag{2}$$

where ΔP_o is the differential pressure between the wellbore pressure and the far-field (undisturbed) pore pressure; B is a factor determined by the dimensions and permeabilities of the mud-formation system. They are expressed as

$$\Delta P_o = P_i - P_e \tag{3}$$

$$B = \frac{K_2 \ln\frac{R_o}{R_i}}{K_1 \ln\frac{R_e}{R_o} + K_2 \ln\frac{R_o}{R_i}} \tag{4}$$

Next, the pore pressure in the formation around the wellbore can be determined. Define P_r as the pore pressure in the formation at distance r ($R_o \le r \le R_e$) from the wellbore center. The following equation can be written from Darcy's law

$$\frac{2\pi K_2}{\mu_2 \ln\frac{r}{R_o}}(P_r - P_o) = \frac{2\pi K_2}{\mu_2 \ln\frac{R_e}{r}}(P_e - P_r) \tag{5}$$

Inserting the pore pressure P_o at the wellbore wall (Eq. (2)) into Eq. (5), the pore pressure P_r at the radial distance r from the wellbore center can be obtained as

$$P_r = P_i - M\Delta P_o \tag{6}$$

where

$$M = \frac{1}{\ln\frac{R_e}{R_o}}\left(\ln\frac{r}{R_o} + \frac{K_2 \ln\frac{R_o}{R_i}\ln\frac{R_e}{r}}{K_1 \ln\frac{R_e}{R_o} + K_2 \ln\frac{R_o}{R_i}}\right) \tag{7}$$

2.1.2 Total stresses around the wellbore induced by varying pore pressure distribution

For the plane-strain circular wellbore model, the total radial and tangential (hoop) stresses around the wellbore induced by varying pressure can be determined by (Fjar et al. 2008)

$$\sigma_{r,p} = \frac{2\eta}{r^2}\left(\int_{R_o}^{r} r'\Delta P(r')\mathrm{d}r' - \frac{r^2 - R_o^2}{R_e^2 - R_o^2}\int_{R_o}^{R_e} r'\Delta P(r')\mathrm{d}r'\right) \tag{8}$$

$$\sigma_{\theta,p} = -\frac{2\eta}{r^2}\left(\int_{R_o}^{r} r'\Delta P(r')\mathrm{d}r' - r^2\Delta P(r) + \frac{r^2 + R_o^2}{R_e^2 - R_o^2}\int_{R_o}^{R_e} r'\Delta P(r')\mathrm{d}r'\right) \tag{9}$$

where $\sigma_{r,p}$ and $\sigma_{\theta,p}$ are the total radial and tangential stresses around the wellbore induced by varying pore pressure; η is the poroelastic stress coefficient; $\Delta P(r) = P_r - P_e$ is the pore pressure difference between location r and far field; combining Eqs. (2) and (6), $\Delta P(r)$ can be expressed as

$$\Delta P(r) = \left(1 - A\ln\frac{r}{R_o} - AB\ln\frac{R_e}{r}\right)\Delta P_o \tag{10}$$

where $A = \frac{1}{\ln\frac{R_e}{R_o}}$; B is defined in Eq. (4).

Define the two integration terms appearing in Eqs. (8) and (9) as

$$I_1 = \int_{R_o}^{r} r'\Delta P\left(r'\right)\mathrm{d}r' \tag{11}$$

$$I_2 = \int_{R_o}^{R_e} r'\Delta P\left(r'\right)\mathrm{d}r' \tag{12}$$

Inserting Eq. (10) into Eqs. (11) and (12) and doing the integrations, I_1 and I_2 can be determined as

$$I_1 = \left\{\left[\frac{r'^2}{2}\right]_{R_o}^{r} - A\left[\frac{1}{4}r'^2\left(2\ln\frac{r'}{R_o} - 1\right)\right]_{R_o}^{r} - AB\left[\frac{1}{4}r'^2\left(2\ln\frac{R_e}{r'} + 1\right)\right]_{R_o}^{r}\right\}\Delta P_o \tag{13}$$

$$I_2 = \left\{\left[\frac{r'^2}{2}\right]_{R_o}^{R_e} - A\left[\frac{1}{4}r'^2\left(2\ln\frac{r'}{R_o} - 1\right)\right]_{R_o}^{R_e} - AB\left[\frac{1}{4}r'^2\left(2\ln\frac{R_e}{r'} + 1\right)\right]_{R_o}^{R_e}\right\}\Delta P_o \tag{14}$$

Inserting Eqs. (13) and (14) into Eqs. (8) and (9), the total radial and tangential stresses around the wellbore induced by varying pore pressure can be expressed as

$$\sigma_{r,p} = \frac{2\eta}{r^2}\left(I_1 - \frac{r^2 - R_o^2}{R_e^2 - R_o^2}I_2\right) \tag{15}$$

$$\sigma_{\theta,p} = -\frac{2\eta}{r^2}\left(I_1 - r^2\Delta P(r) + \frac{r^2 + R_o^2}{R_e^2 - R_o^2}I_2\right) \tag{16}$$

2.2 Total stresses around the wellbore induced by wellbore pressure, far-field stresses and plastic mudcake

2.2.1 Kirsch solutions

Because the mudcake is usually very soft/flexible compared to the formation, it is reasonable to assume that the mudcake does not exert any shear tractions on the wellbore wall (Tran et al. 2011). Radial mechanical pressure is the only force applied to the wellbore wall by the mudcake. Under this condition, the Kirsch solutions are still valid. Therefore, the total stress around wellbore induced by the far-field stresses and the mechanical pressure on wellbore wall can be determined as

$$\sigma_{r,s+w} = \frac{\sigma_H + \sigma_h}{2}\left(1 - \frac{R_o^2}{r^2}\right) + \frac{\sigma_H - \sigma_h}{2}\left(1 + 3\frac{R_o^4}{r^4} - 4\frac{R_o^2}{r^2}\right)\cos 2\theta + P_{iw}\frac{R_o^2}{r^2} \tag{17}$$

$$\sigma_{\theta,s+w} = \frac{\sigma_H + \sigma_h}{2}\left(1 + \frac{R_o^2}{r^2}\right) - \frac{\sigma_H - \sigma_h}{2}\left(1 + 3\frac{R_o^4}{r^4}\right)\cos 2\theta - P_{iw}\frac{R_o^2}{r^2} \tag{18}$$

where $\sigma_{r,s+w}$ and $\sigma_{\theta,s+w}$ are the total radial and tangential stresses around wellbore induced by far-field stresses superposed on the mechanical pressure on the wellbore wall exerted by mudcake; θ is the circumferential angle to the direction of σ_H, as shown in Fig. 1; P_{iw} is the pressure exerted on wellbore wall by the mudcake. It should be noted that P_{iw} is not equal to wellbore pressure P_i acting on the inner surface of mudcake; rather, it is influenced by the fluid flow through the mudcake and the plastic flow of the mudcake itself.

2.2.2 Stress applied on the wellbore wall by the mudcake

For the plain strain problem considered in this study, the equations of equilibrium for the mudcake can be simplified to a single equation in cylindrical coordinates (Fjar et al. 2008)

$$\frac{\mathrm{d}\sigma_{r,c}}{\mathrm{d}r} + \frac{\sigma_{r,c} - \sigma_{\theta,c}}{r} = 0 \tag{19}$$

where $\sigma_{r,c}$ and $\sigma_{\theta,c}$ are the radial and tangential stresses in the mudcake, respectively. The stress–strain relationships for the mudcake can be expressed as

$$\begin{aligned} E_c\varepsilon_{r,c} &= \sigma_{r,c} - \nu_c\left(\sigma_{\theta,c} + \sigma_{z,c}\right) \\ E_c\varepsilon_{\theta,c} &= \sigma_{\theta,c} - \nu_c\left(\sigma_{r,c} + \sigma_{z,c}\right) \\ E_c\varepsilon_{z,c} &= \sigma_{z,c} - \nu_c\left(\sigma_{r,c} + \sigma_{\theta,c}\right) \end{aligned} \tag{20}$$

where E_c and ν_c are the Young's modulus and Poisson's ratio of the mudcake, respectively; $\varepsilon_{r,c}$, $\varepsilon_{\theta,c}$, and $\varepsilon_{z,c}$ are the radial, tangential, and axial strains of the mudcake, respectively; $\sigma_{z,c}$ is the axial stress in the mudcake.

Due to its very soft/flexible features, the mudcake can be assumed to be in a perfectly plastic-yielding condition with a small yield strength under the differential pressure between the wellbore and the formation (Tran et al. 2011). Poisson's ratio for mudcake plastic flow is assumed to be 0.5. The mudcake is considered in a plane-strain condition; thus $\varepsilon_{z,c} = 0$. Then, from the last equation of Eq. (20), one can get

$$\sigma_{z,c} = 0.5\left(\sigma_{r,c} + \sigma_{\theta,c}\right) \tag{21}$$

According to the von Mises yield theory (also known as maximum distortion energy theory), the following expression can be found when the mudcake yields (Aadnøy and Belayneh 2004)

$$Y = \sqrt{\frac{1}{2}\left[\left(\sigma_{r,c} - \sigma_{\theta,c}\right)^2 + \left(\sigma_{r,c} - \sigma_{z,c}\right)^2 + \left(\sigma_{\theta,c} - \sigma_{z,c}\right)^2\right]} \tag{22}$$

where Y is the yield strength of the mudcake.

Inserting Eq. (21) into Eq. (22), one can get

$$Y = \frac{\sqrt{3}}{2}\left(\sigma_{\theta,c} - \sigma_{r,c}\right) \tag{23}$$

Inserting Eq. (23) into the equilibrium equation (Eq. (20)), the radial stress distribution in the mudcake can be expressed as

$$\sigma_{r,c} = \frac{2Y}{\sqrt{3}}\ln(r) + C \tag{24}$$

where C is an integration constant.

Applying the boundary condition at the inner mudcake surface $\sigma_{r,c|r=R_i} = P_i$ into Eq. (24), the integration constant C can be determined as

$$C = P_i - \frac{2Y}{\sqrt{3}}\ln(R_i) \tag{25}$$

Inserting Eq. (25) into Eq. (24), the radial stress distribution in the mudcake can be determined as

$$\sigma_{r,c} = P_i - \frac{2Y}{\sqrt{3}}\ln\left(\frac{r}{R_i}\right) \tag{26}$$

where $R_i \le r \le R_o$.

On the wellbore wall $r = R_o$, the radial stress is

$$\sigma_{r,c|r=R_o} = P_i - \frac{2Y}{\sqrt{3}}\ln\frac{R_o}{R_i} \tag{27}$$

As aforementioned, it is reasonable to assume that the mudcake does not exert any shear traction on the wellbore wall because it is extremely soft/flexible compared to the formation (Tran et al. 2011). However, the mudcake can transmit part of the radial stress exerted by the wellbore fluid on the inner surface of mudcake to the wellbore wall, depending on the yield strength and thickness of the mudcake. The radial stress on the inner surface of the mudcake is equal to drilling fluid pressure P_i, while the radial stress on the wellbore wall is given by Eq. (27). Therefore, by simply replacing P_{iw} in the Kirsch solutions (Eqs. 17 and 18) with $\sigma_{r,c|r=R_o}$ (Eq. (27)), the total stress around the wellbore induced by wellbore pressure, far-field stress, and plasticity of mudcake can be determined as

$$\begin{aligned}\sigma_{r,s+w} = {} & \frac{\sigma_H + \sigma_h}{2}\left(1 - \frac{R_o^2}{r^2}\right) \\ & + \frac{\sigma_H - \sigma_h}{2}\left(1 + 3\frac{R_o^4}{r^4} - 4\frac{R_o^2}{r^2}\right)\cos 2\theta + P_i\frac{R_o^2}{r^2} \\ & - \frac{2Y}{\sqrt{3}}\ln\left(\frac{R_o}{R_i}\right)\frac{R_o^2}{r^2}\end{aligned} \tag{28}$$

$$\begin{aligned}\sigma_{\theta,s+w} = {} & \frac{\sigma_H + \sigma_h}{2}\left(1 + \frac{R_o^2}{r^2}\right) - \frac{\sigma_H - \sigma_h}{2}\left(1 + 3\frac{R_o^4}{r^4}\right)\cos 2\theta \\ & - P_i\frac{R_o^2}{r^2} + \frac{2Y}{\sqrt{3}}\ln\left(\frac{R_o}{R_i}\right)\frac{R_o^2}{r^2}\end{aligned} \tag{29}$$

In Eqs. (28) and (29), the first two terms are the total stress concentration contributed by far-field stresses as a result of the creation of the wellbore; the third term denotes the stress induced by the wellbore pressure; and the last term is the contribution of the mudcake.

2.3 Total stresses around the wellbore

In the above sections, the total stresses induced by varying pore pressure around the wellbore due to fluid flow (Eqs. 15 and 16) and the total stress induced by wellbore pressure, far-field stress, and plasticity of mudcake (Eqs. 28 and 29) have been derived. Assuming these terms are uncoupled, the total stress solutions are therefore a superposition of them

$$\sigma_r = \sigma_{r,p} + \sigma_{r,s+w} \tag{30}$$

$$\sigma_\theta = \sigma_{\theta,p} + \sigma_{\theta,s+w} \tag{31}$$

where σ_r and σ_θ are the total radial and tangential stresses around the wellbore, respectively.

2.4 Effective stresses around wellbore

Effective stresses around the wellbore are equal to total stresses minus pore pressure at the corresponding locations, i.e.,

$$\sigma'_r = \sigma_{r,p} + \sigma_{r,s+w} - P_r \tag{32}$$

$$\sigma'_\theta = \sigma_{\theta,p} + \sigma_{\theta,s+w} - P_r \tag{33}$$

where σ'_r and σ'_θ are the effective radial and tangential stresses around the wellbore; P_r is the pore pressure at distance r from the wellbore center, defined in Eq. (6).

The effective stresses on the wellbore wall ($r = R_o$) can be determined as

$$\sigma'_{r|r=R_o} = \sigma_{r|r=R_o} - P_o \tag{34}$$

$$\sigma'_{\theta|r=R_o} = \sigma_{\theta|r=R_o} - P_o \tag{35}$$

where $\sigma'_{r|r=R_o}$ and $\sigma'_{\theta|r=R_o}$ are the effective radial and tangential stresses on the wellbore wall, respectively; $\sigma_{r|r=R_o}$ and $\sigma_{\theta|r=R_o}$ are the total tangential stresses on the wellbore wall which can be determined by Eqs. (32) and (33), respectively; P_o is the pore pressure on the wellbore wall, defined in Eq. (2).

2.5 Fracture initiation pressure

Fracture initiation occurs when the minimum effective tangential stress on the wellbore wall reaches the tensile strength of the rock. Under non-uniform horizontal stresses as shown in Fig. 1, the minimum effective tangential stress on wellbore wall can be found at $\theta = 0$ or π and determined by Eq. (35) as

$$\sigma'_{\theta,\min} = 3\sigma_h - \sigma_H - P_i + \frac{2Y}{\sqrt{3}}\ln\left(\frac{R_o}{R_i}\right) + \sigma_{\theta,p|r=R_o} - P_o \tag{36}$$

where $\sigma_{\theta,p|r=R_o}$ is the total tangential stress on the wellbore wall induced by the varying pore pressure and can be determined by Eq. (16) as

$$\sigma_{\theta,p|r=R_o} = -2\eta(M-N)(P_i - P_e) \tag{37}$$

where M and N are functions of the geometry and permeability of the wellbore-mudcake system in Fig. 1

$$M = 1 - \frac{2A}{R_e^2 - R_o^2}\left[\frac{1}{4}R_e^2\left(2\ln\frac{R_e}{R_o} - 1\right) + \frac{1}{4}R_o^2\right] - \frac{2AB}{R_e^2 - R_o^2}\left[\frac{1}{4}R_e^2 - \frac{1}{4}R_o^2\left(2\ln\frac{R_e}{R_o} + 1\right)\right] \tag{38}$$

$$N = \left(1 - AB\ln\frac{R_e}{R_o}\right) \tag{39}$$

A and B are the same as defined in Sect. 2.1.

The tensile strength of the rock is assumed to be zero in this study in order to simplify the analyses in the later sections. Therefore, fracture occurs when

$$\sigma'_{\theta,\min} = 0 \tag{40}$$

Combining Eqs. (40), (36), (37), and (2), the fracture initiation pressure (i.e., the minimum wellbore pressure at which a fracture occurs on the wellbore wall) for a wellbore with a mudcake can be determined as

$$P_f = \frac{3\sigma_h - \sigma_H + [2\eta(M-N) - B]P_e + \frac{2Y}{\sqrt{3}}\ln\frac{R_o}{R_i}}{2 + 2\eta(M-N) - B} \tag{41}$$

Besides far-field stresses and formation pore pressure, this solution also takes into account the effects of mudcake parameters on FIP, including mudcake permeability, thickness, and strength. In the following sections, the effects of mudcake parameters on FIP and distributions of near-wellbore stresses and pore pressure are illustrated through numerical examples. In addition, the implications of the analysis results on wellbore strengthening for lost circulation prevention are discussed.

It should be noted again that, due to the complexity of the mudcake problem, the current model assumes steady-state fluid flow, and thus the transient pore pressure effect on wellbore strengthening is not considered. Further improvement of the model to include transient effects can use the decomposition scheme for time-dependent poroelastic solution of a borehole without mudcake proposed by Cui et al. (1997). However, more complicated mathematical derivations will be involved due to the introduction of mudcake to the problem. In Cui's study, the transient problem was decomposed to three linear problems, namely a poroelastic plane-strain problem, an elastic uniaxial stress problem, and an elastic anti-plane shear problem. Due to the linearity of the problems, the final solution can be obtained by the superposition principle. Readers are referred to Cui et al. (1997, 1999) for more details of the decomposition approach.

3 Effects of mudcake parameters

Recent experimental studies on wellbore strengthening have revealed the important role of mudcake on inhibiting the growth of fractures that would otherwise cause lost circulation (Cook et al. 2016; Guo et al. 2014; Salehi and Kiran 2016). A thorough understanding of the effects of mudcake parameters on near-wellbore stress profiles and FIP is critical for mud design to obtain optimal mudcake during drilling. The analytical analysis in Sect. 2 indicates that mudcake alters the stress profile and FIP through its thickness, permeability, and strength. In this section, the effects of these parameters are quantitatively illustrated with a parametric study.

Mudcake parameters are very difficult to measure in field drilling operations. Hence, they are usually determined from laboratory experiments. Filtration tests are the most commonly used approach. There are two categories of filtration tests: static and dynamic tests (Jaffal et al. 2017). In static tests, the mud in contact with the formation is stagnant and the mudcake forms due to the deposition of mud particles. Whereas in dynamic filtration tests, the mud is flowing across the face of the formation, and therefore the mudcake results from the dynamic equilibrium between the deposition rate and erosion rate (due to shear stress generated by fluid flow) of mud particles. Mudcake thickness is usually measured using the traditional, direct method with a caliper (Bageri et al. 2013). To eliminate direct contact and damage of mudcake, laser apparatus was used as a non-contact approach to measure mudcake

thickness (Amanullah and Tan, 2000). Mudcake permeability cannot be measured directly, so it must be calculated with a filtration model, together with filtration data measured in the test which usually includes filtrate volume, filtration time, and pressure drop across the mudcake. Chenevert and Dewan (2001) proposed a model to determine mudcake permeability using static filtration data, which was further improved recently by Jaffal et al. (2017). Dangou and Chandler (2009) proposed a model for mudcake permeability evaluation based on dynamic filtration data.

Yield strength of mudcake is more difficult to measure. A major problem in measuring the yield strength of a soft mudcake using conventional rheometers is the slippage between the material and the rheometer parts which contact the material (Bailey et al. 1998). The vane method has been used to measure mudcake strength in which a bladed vane sensor is inserted into the material and rotated until the torque reaches a maximum. The yield strength can then be obtained from its relationship with the measured torque (Meeten and Sherwood 1992). Other methods for measurement of mudcake strength include the squeeze-film method (Sherwood et al. 1991), hole-punch method (Bailey et al. 1998), and scratch test (Berntsen et al. 2010; Cerasi et al. 2001). For a comprehensive review of the techniques for measuring mudcake properties, readers are referred to Bageri et al. (2013).

The ranges of mudcake parameters (i.e., thickness, permeability, and strength) used in the numerical examples are selected from a review of published experimental data, which will be further illustrated in the following subsections. A set of base-case mudcake parameters as well as other parameters of the mudcake-wellbore system are reported in Table 1. In the following parametric analyses, parameters identical with the base-case ones are used unless otherwise specified.

Table 1 Base-case parameters for the numerical examples

Parameter	Value
Mudcake thickness, mm	2
Mudcake permeability, mD	0.01
Mudcake yield strength, MPa	0.15
Formation permeability, mD	1
Wellbore radius, m	0.1
Model outer radius, m	1
Maximum horizontal stress, MPa	22
Minimum horizontal stress, MPa	18
Formation pressure, MPa	10
Wellbore pressure, MPa	12
Wellbore angle θ, degrees	0
Poroelastic coefficient, η	0.3

3.1 Effect of mudcake thickness

Mudcake thickness is influenced by a number of factors, including pressure difference between wellbore and formation, mud flow regimes, mud characteristics, formation porosity and permeability, etc. There is a large literature on measurements of mudcake thickness, but the range of mudcake thickness reported is not consistent. Bezemer and Havenaar (1966) tested mudcake buildup under dynamic mud circulation condition and found that mudcake can build up to 3 mm under low shear rate conditions and 1.8 mm at high shear rate conditions. Griffith and Osisanya (1999) measured mudcake thickness for muds with different filtration loss capacity and found that mudcake thickness can increase up to 6 and 1 mm for high and low filtration loss mud, respectively. Jaffal et al. (2017) provided mudcake thickness data under static filtration conditions and the maximum thickness obtained is about 5 mm. Liu and Civan (1994) found that the mudcake can grow up to 4 mm under low overbalance pressure conditions and to 1.6 mm under high overbalance pressure conditions. Badrul et al. (2007) measured the mudcake thickness for muds with various contents of dolomite as a weighting agent. They concluded that mudcake thickness increases with an increase in dolomite content and a 1.14-cm-thick mudcake was obtained with a high dolomite content. Although the mudcake thicknesses measured in the previous studies vary, most of them are less than 1 cm. Therefore, mudcake thickness ranging from 0 to 1 cm is assumed in this section for investigating its influence on wellbore stress and FIP.

Mudcake thickness affects wellbore stress and consequently FIP through two mechanisms: (1) it influences the near-wellbore pore pressure distribution and thus the stress induced by varying pore pressure (Eqs. 15 and 16), and (2) it affects the magnitude of the radial stress transmitted from the inner mudcake surface to the wellbore wall (Eq. 27).

Figure 2 shows the pore pressure distribution along the radial distance from the wellbore center for different mudcake thicknesses. Two extreme cases of a wellbore with an impermeable mudcake and without mudcake are also included for comparison. The results indicate that the pore pressure in the near-wellbore region decreases with an increase in the mudcake thickness because the mudcake can effectively inhibit fluid flow from the wellbore to the formation. Even with a 2-mm-thin mudcake, the pore pressure in the wellbore vicinity exhibits a significant reduction compared with the case without mudcake.

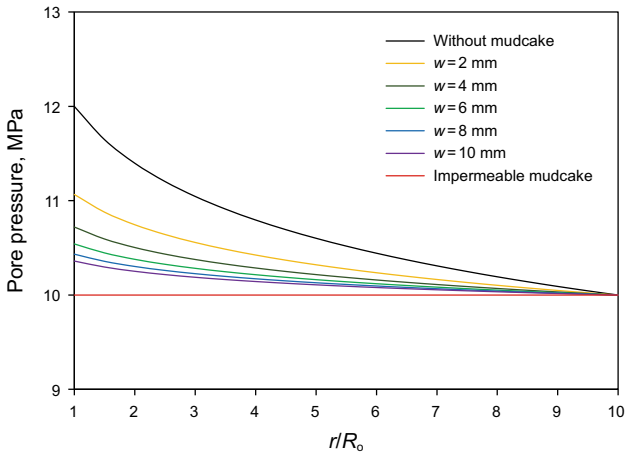

Fig. 2 Pore pressure distribution along the radial direction for different mudcake thicknesses

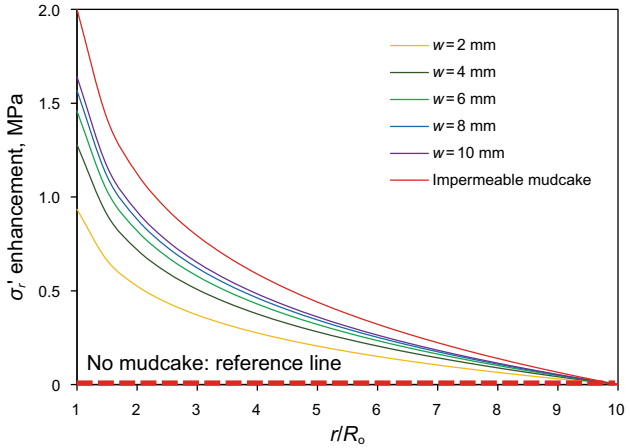

Fig. 3 Enhancement of the effective radial stress along the σ_H direction for different mudcake thicknesses compared to the case without mudcake

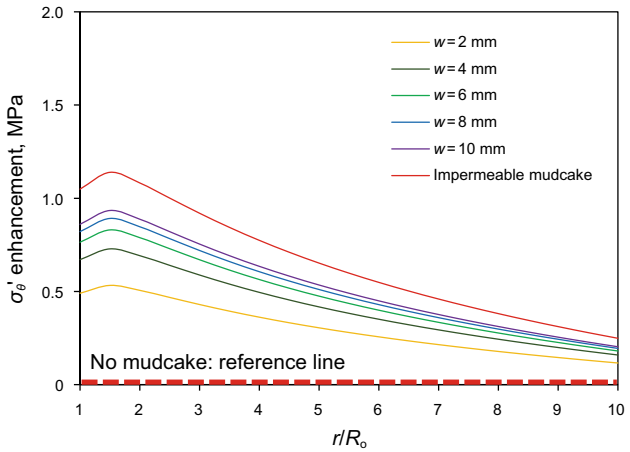

Fig. 4 Enhancement of effective tangential stress along the σ_H direction for different mudcake thicknesses compared to the case without mudcake

Figures 3 and 4 show the effects of mudcake thickness on radial and tangential stresses along the direction of the maximum horizontal stress σ_H (the most likely direction for fracture extension). The figures present enhancements of the effective stresses for a wellbore with a permeable mudcake with reference to the case without any mudcake. The extreme case for the wellbore with an impermeable mudcake is also included for comparison, which is the ideal condition with the least likelihood of tensile fracture or lost circulation. The results show that both radial and tangential stresses increase with a mudcake on the wellbore compared with the case without mudcake. With an increase in the mudcake thickness, the stress enhancement increases. Even with the presence of a very thin mudcake (e.g., 2 mm), the tangential stress can be effectively elevated by about 0.6 MPa in the near-wellbore region, implying effective strengthening of the wellbore. With a relatively thick mudcake (e.g., 8 or 10 mm), the tangential stress enhancement increases up to about 1 MPa, and the wellbore stress approaches the condition with an impermeable mudcake.

Figure 5 shows the predicted FIP for different mudcake thicknesses. It can be observed that FIP has a significant enhancement with an increase in the mudcake thickness, implying that the wellbore can be better strengthened by a thicker mudcake. In this particular case, FIP can be increased by 1.5 MPa with a 2-mm-thin mudcake and by 3 MPa with a relatively thick mudcake of 1 cm. This result qualitatively agrees with the observation of experimental studies that a mudcake can effectively increase the sustainable pressure of a wellbore and reduce the risk of lost circulation (Cook et al. 2016). Although a thicker mudcake is beneficial for preventing lost circulation, it has several demerits, such as reducing the efficient well diameter, excessive torque and drag when rotating or pulling the drilling string, stuck pipe, etc. Therefore, a thicker

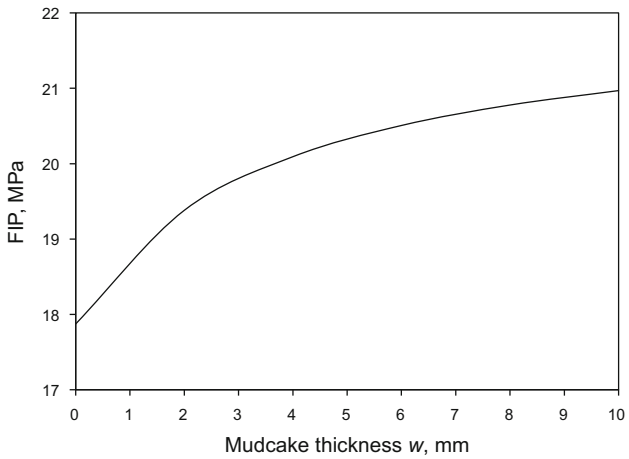

Fig. 5 FIP for different mudcake thicknesses

mudcake is usually not recommended in drilling operations. Fortunately, mudcake permeability can be manipulated by engineering the drilling mud formulations to achieve optimal wellbore strengthening performance with a thinner mudcake.

As mentioned earlier, the mudcake thickness impacts the stress profile and FIP through two mechanisms: altering the pore pressure around the wellbore and the radial stress transmitted to the wellbore wall across the mudcake. The magnitude of the stress perturbation σ_{mc} due to the latter mechanism is the last term in Eqs. (20) or (29), i.e.,

$$\sigma_{mc}=\frac{2Y}{\sqrt{3}}\ln\left(\frac{R_o}{R_i}\right)\frac{R_o^2}{r^2} \tag{42}$$

Considering the typical range of the wellbore radius R_o from 0.1 to 0.13 m (Tran et al. 2011) and the typical range of the mudcake thickness from 0 to 0.01 m (Bezemer and Havenaar 1966; Chenevert and Dewan 2001; Griffith and Osisanya 1999; Sepehrnoori et al. 2005), the range of the inner mudcake radius R_i is between 0.09 and 0.13 m and the value of the term $\ln(R_o/R_i)$ is very small, less than 0.1. Because the mudcake yield strength Y is also small, typically less than 1 MPa (Cerasi et al. 2001; Cook et al. 2016) and the term $\frac{R_o^2}{r^2}$ is less than 1, the magnitude of stress perturbation σ_{mc} induced by the mudcake is very small and typically less than 0.1 MPa. Therefore, it can be concluded that the mudcake increases the wellbore hoop stress and FIP mainly through modifying fluid flow and consequently the pore pressure distribution around the wellbore, rather than changing the radial stress transmission across the mudcake to the wellbore wall. The effect of mudcake strength will be further discussed in later sections.

3.2 Effect of mudcake permeability

Permeability of the mudcake is another important parameter, controlling fluid flow through the mudcake and pore pressure variation around the wellbore. Similar to the mudcake thickness, the mudcake permeability is also influenced by many factors, such as formation porosity and permeability, differential pressure across the mudcake, and particle type and size in the mud. The range of mudcake permeability measured in the previous studies also varies. According to the dynamic filtration tests by Bezemer and Havenaar (1966), the mudcake permeability can range between 2×10^{-4} and 5×10^{-4} mD dependent on the rate of shear on the mudcake surface. Chenevert and Dewan (2001) reported that the mudcake permeability can range from 10^{-4} to 10^{-2} mD for different pressures across the mudcake. Griffith and Osisanya (1999) found that the mudcake permeability can be as low as several nano-Darcy in dynamic filtration tests. Sepehrnoori et al. (2005) indicated that the mudcake permeability can quickly stabilize at 10^{-3}–10^{-2} mD after a few seconds of filtration. Jaffal et al. (2017) measured, under static filtration conditions, mudcake permeability which ranges from 10^{-3} to 10^{-1} mD. From the literature review, it is found that 10^{-4}–10^{-2} mD is a typical range for mudcake permeability which will be adopted in the parametric analysis in this section.

Figure 6 presents the effect of mudcake permeability on the pore pressure around the wellbore. The pore pressure distributions without mudcake and with impermeable mudcake are also included for comparison. The results show that the pore pressure around the wellbore decreases with a reduction in the mudcake permeability. When the mudcake permeability is as low as 10^{-4} mD, the pore pressure around the wellbore is almost identical to the formation pressure and approaches the condition of an impermeable well.

Figures 7 and 8 show the enhancements of effective radial and tangential stresses in the σ_H direction for wellbore with a permeable mudcake with reference to the case without mudcake. The results show that both radial and tangential stresses increase with a decrease in the mudcake permeability. With a very low mudcake permeability, e.g., 10^{-3} mD, the stresses become very close to those of an impermeable wellbore, implying a lower risk of lost circulation.

The effect of mudcake permeability on FIP of the wellbore is shown in Fig. 9. The results show that FIP decreases dramatically with an increase in the mudcake permeability. When compared with the case without mudcake, a 10^{-2} mD mudcake can lead to a 1 MPa increase in FIP and a 10^{-3} mD mudcake can cause as much as a 2 MPa increase in FIP. Hence, decreasing mudcake permeability can effectively reduce the likelihood of

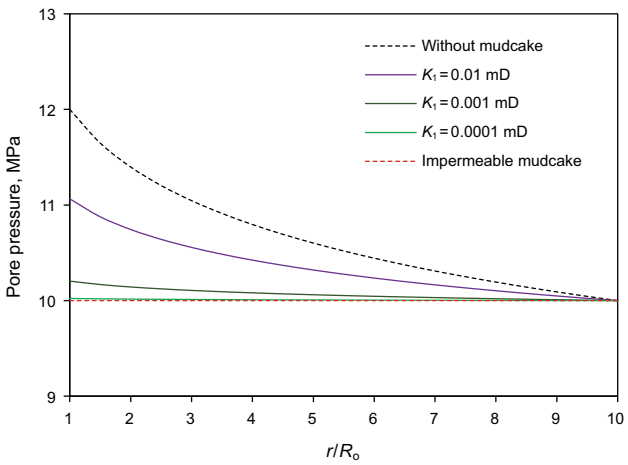

Fig. 6 Pore pressure distribution along the radial direction for different mudcake permeabilities

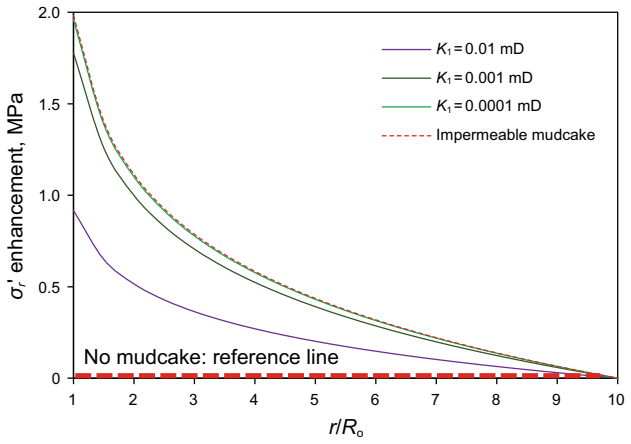

Fig. 7 Enhancement of effective radial stress along the σ_H direction for different mudcake permeabilities compared to the case without mudcake

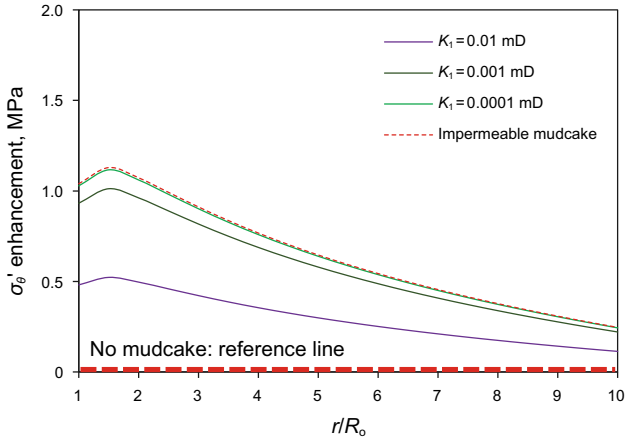

Fig. 8 Enhancement of effective tangential stress along the σ_H direction for different mudcake permeabilities compared to the case without mudcake

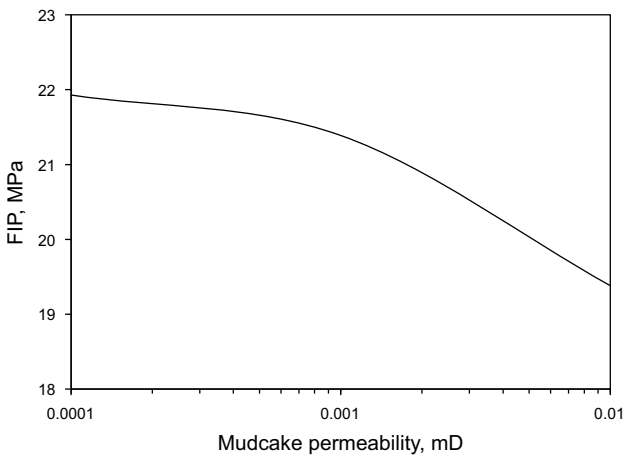

Fig. 9 FIP for different mudcake permeabilities

wellbore fracturing. However, despite the low permeability of the mudcake, e.g., 10^{-3} mD, the FIP with a permeable mudcake is still much lower than that of an impermeable wellbore. Therefore, neglecting the permeable nature of the mudcake (i.e., assuming it is impermeable) may lead to substantial overestimation of the FIP. The calculation results suggest that, in wellbore strengthening operations, it is critical to properly engineer the mud formulations to build a tight, low-permeability mudcake on the wellbore wall. In addition, a tight mudcake is also beneficial for mitigating problems of wellbore instability and formation damage.

3.3 Effect of mudcake strength

The contribution of mudcake strength on wellbore stress profiles is reflected in Eq. (42). From the discussion in the last paragraph in Sect. 3.1, it can be seen that this contribution should be very small. Even though experimental studies have revealed a wide range in mudcake yield strength, the values are all quite small. Bailey et al. (1998) have shown that yield strength of mudcake ranges from 0.1 to 1 MPa and is a function of water content and solids volume fraction of the mud. Cook et al. (2016) have reported that the mudcake yield strength is a function of applied differential pressure and mud type: for oil-based muds, the mudcake yield strength can increase from 0.2 to 0.6 MPa as the differential pressure increases from 0.5 to 3 MPa; for water-based muds, the yield strength can increase from 0.4 to 1.7 MPa with the same differential pressure increase. The mudcake formed from oil-based muds is usually weaker than that formed from water-based muds (Cook et al. 2016).

Figures 10 and 11 show the effective tangential stress profile and FIP of the wellbore for mudcake with a yield stress of 1 and 0 MPa (extreme case). A comparison

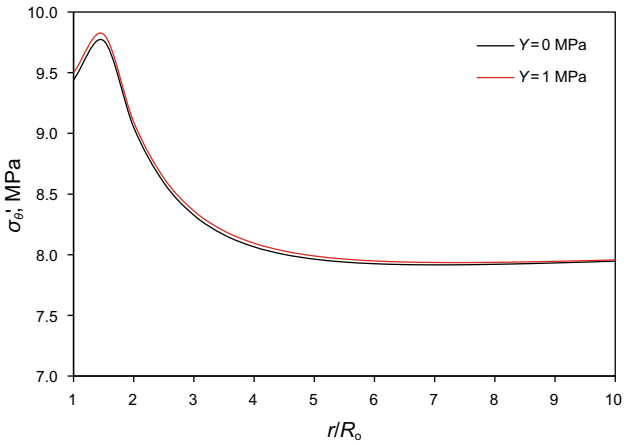

Fig. 10 Effective tangential stress around the wellbore with different mudcake yield strengths

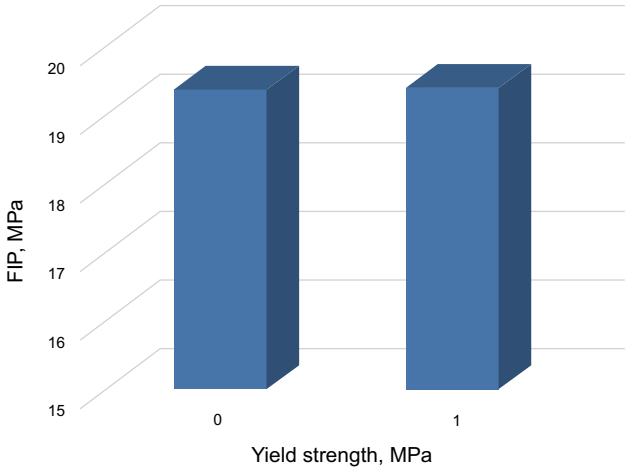

Fig. 11 FIP with different mudcake yield strengths

between the two cases shows that the effects of mudcake strength are negligibly small. Therefore, it can be concluded that mudcake increases the FIP mainly through preventing/mitigating fluid seepage from wellbore to the surrounding formation and consequently inhibiting the development of tensile stress around the wellbore. However, the negligible effect of mudcake strength on FIP does not mean that the mudcake strength is not important for preventing fluid loss, which will be explained in detail in the following section.

It should be noted that above analyses are based on the assumption of an intact wellbore without pre-existing natural fractures or induced fractures on the wellbore wall. It is well known that a wellbore with pre-existing fractures usually has lower FIP due to the loss of wellbore tensile strength (Feng et al. 2016). For most sedimentary formations, FIP of a wellbore decreases quickly with the length of pre-existing fractures. A fracture-mechanics-based model for predicting FIP of a wellbore with pre-existing fractures (but with no mudcake) can be found in Lee et al. (2004).

Even though the presented model does not consider pre-existing fractures, it still adds value to the study of wellbore strengthening. Most wellbore strengthening models focus on the investigation of bridging or plugging fractures on the wellbore. However, not all wellbores have initially well-developed fractures. In such scenarios, mudcake has an important role in stabilizing the wellbore. Field evidence is: (1) it is well known that compared with the water-based mud (WBM), the oil-based mud (OBM) usually has poor mudcake development due to minimal leak-off. As a result, lost circulation (wellbore fracturing) events occur more frequently with OBM due to the lack of mudcake. (2) Poroelasticity theory has shown that, with no mudcake, clean sandstones (with relatively high permeability) usually have lower FIP compared with silty shale (mixture of shale and sand with relatively low permeability). However, field practices have shown that lost circulation occurs more frequently in silty shales than in clean sandstones because of poor mudcake development (Ziegler and Jones 2014). In addition, theoretical studies of Tran et al. (2011) have indicated that a mudcake can increase fracture pressure by 16%, compared to the case without mudcake. When pre-existing fractures exist, mudcake can still have an important role in preventing fluid loss, as will be discussed in Sect. 5.

4 Comparison with fracture-bridging wellbore strengthening method

High cost is usually involved in the development of oil and gas projects, especially for offshore projects (Rui et al. 2017a, b, c, 2018). Lost circulation is a major costly incident in the drilling and completion phases. Existing studies have indicated that lost circulation can be effectively mitigated by wellbore strengthening (Alberty and McLean 2004; Arlanoglu et al. 2014; Zhao et al. 2017). The above analysis has shown that increased FIP and thus wellbore strengthening can be achieved by forming a mudcake on the wellbore wall. Another major method in the drilling industry to strengthen a wellbore is the technique based on bridging fractures on the wellbore wall (Alberty and McLean 2004; Feng et al. 2015; Feng and Gray 2016a; Song and Rojas 2006). In this section, wellbore strengthening effects created by a mudcake and by the fracture-bridging method are compared. FIP of the wellbore is used as a criterion for the comparison, i.e., the higher the FIP, the better the strengthening result.

The common practice of the fracture-bridging method (e.g., the stress-cage method) is to create a small fracture on the wellbore wall and then bridge the fracture with LCMs to increase the pressure bearing capacity of the wellbore (Alberty and McLean 2004; Morita and Fuh 2012). For this method, Feng and Gray (2016b) developed an analytical solution based on linear elastic mechanics to predict FIP after bridging two small fractures extending symmetrically from the wellbore wall and perpendicular to σ_h, as shown in Fig. 12. The solution is expressed as:

$$P_f = \frac{1}{2}\cdot\frac{1}{F_1+F_2-F_4}\cdot K_{IC} + \frac{1}{2}\cdot\frac{F_1+F_2}{F_1+F_2-F_4}\cdot(\sigma_H+\sigma_h) - \frac{1}{2}\cdot\frac{F_1+3F_3}{F_1+F_2-F_4}\cdot(\sigma_H-\sigma_h) - \frac{F_4}{F_1+F_2-F_4}\cdot P_p \quad (42)$$

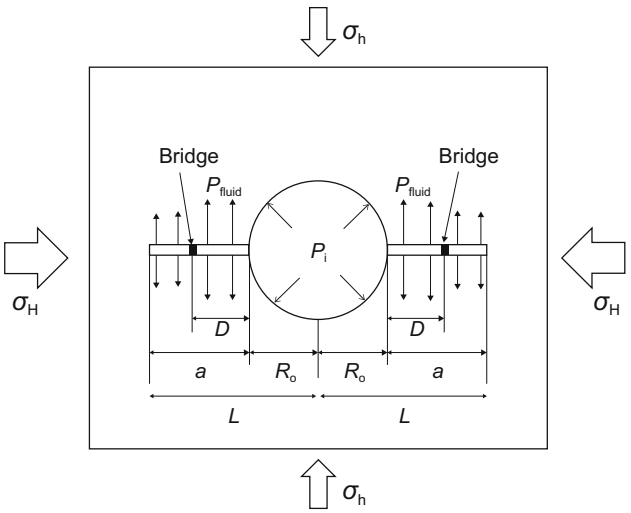

Fig. 12 Bridging of two symmetric fractures in wellbore strengthening (modified after Feng and Gray 2016b)

$$F_1 = \frac{1}{\sqrt{\pi a}} \int_{R_o}^{L} G(r)\mathrm{d}r$$

$$F_2 = \frac{1}{\sqrt{\pi a}} \int_{R_o}^{L} \frac{R_o^2}{r^2} G(r)\mathrm{d}r$$

$$F_3 = \frac{1}{\sqrt{\pi a}} \int_{R_o}^{L} \frac{R_o^4}{r^4} G(r)\mathrm{d}r$$

$$F_4 = \frac{1}{\sqrt{\pi a}} \int_{D}^{L} G(r)\mathrm{d}r$$

$$G(r) = \frac{1.3 - 0.3\left(\frac{r-R_o}{a}\right)^{5/4}}{\sqrt{1 - \left(\frac{r-R_o}{a}\right)^2}}$$

where P_f is FIP of the wellbore after bridging the fractures; K_{IC} is the fracture toughness of the rock; F_1, F_2, F_3, and F_4 are factors dependent on the geometry of the wellbore-fracture system; R_o is the wellbore radius; L is the distance from the wellbore center to the fracture tip; a is the fracture length; and D is the LCM bridge location.

It should be noted that in the fracture-bridging model, the fracture toughness of rock is involved, which, however, cannot be directly used in the continuum-mechanics model developed in this paper. Fortunately, numerous existing studies have shown that there is a strong relation between fracture toughness and tensile strength of rocks (Haberfield and Johnston 1989; Khan and Al-Shayea 2000; Whittaker et al. 1992; Zhang et al. 1998; Zhang 2002) and the later can be easily incorporated into the FIP solution (Eq. 41) in this paper by simply adding a tensile strength term to the numerator of Eq. (41). In this section, the following equation proposed by Zhang (2002) based on extensive experimental results is used to correlate these two parameters:

$$S_t = 6.88K_{IC} \tag{43}$$

where S_t is the tensile strength of rock; 6.88 is the correlation coefficient.

Input data in Table 2 are used for the comparison between the mudcake model and the fracture-bridging model for wellbore strengthening. The stress and rock properties are consistent with those used in Feng and Gray (2016b). For the fracture-bridging model, the commonly used 0.15-m (6-in) fracture length assumption is adopted (Alberty and McLean 2004; Arlanoglu et al. 2014; Aston et al. 2007; Wang et al. 2009). The tensile strength is 15 MPa determined from the fracture toughness using Eq. (43). The mudcake is assumed to have a constant permeability of 0.01 mD.

With above parameters, Fig. 13 shows FIPs obtained from the mudcake model (with different mudcake thicknesses) and from the fracture-bridging model (with different bridging locations). Note that the bottom horizontal axial is normalized mudcake thickness with a maximum thickness w_{max} of 10 mm, i.e., the mudcake thickness varies from 0 (no mudcake) to 10 mm. The top horizontal axial is normalized bridging location D (see Fig. 12) with fracture length a; therefore, $D/a = 0$ means the fracture is bridged at the wellbore wall, while $D/a = 1$ means the fracture is bridged at the very tip of the fracture (equivalent to the case without bridging). The results show that, for an intact wellbore with no fracture and mudcake ($w/w_{max} = 0$), FIP is 30.3 MPa; while after creating a 0.15-m fracture, FIP reduces to 22.3 MPa (at $D/a = 1$). For mudcake-based wellbore strengthening, FIP is increased by 23.3% with a very thick mudcake of 10 mm and by 16.7% with a moderate mudcake thickness of 4 mm. For wellbore strengthening based on fracture-bridging, FIP can be increased beyond that of an intact wellbore only when the

Table 2 Base input parameters used for model comparison

Parameter	Value
Wellbore radius, m	0.15
Fracture length, m	0.15
Minimum horizontal stress, MPa	24.82
Maximum horizontal stress, MPa	20.68
Pore pressure, MPa	12.41
Fracture toughness, MPa-m$^{0.5}$	2.2
Tensile strength, MPa	15
Rock permeability, mD	1
Mudcake permeability, mD	0.01

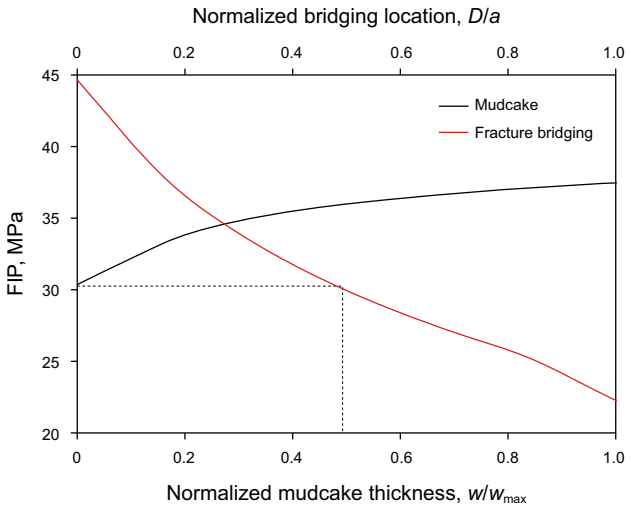

Fig. 13 Comparison of FIP with mudcake-based and fracture-bridging-based wellbore strengthening methods

bridging location is relatively close to the wellbore wall (i.e., $D/a < 0.5$). If the fracture can be perfectly bridged at the immediate wellbore wall, a significant increase of 46% in FIP (compared to intact wellbore case) can be achieved. However, field practices have shown that it is always difficult to bridge the fracture at the immediate wellbore wall (Zoback 2010). Figure 13 indicates that when $D/a < 0.5$, the fracture-bridging method has a comparable or superior wellbore strengthening effect compared with the mudcake-based method; otherwise, the fracture-bridging method fails to strengthen the wellbore in this particular case.

5 Discussion

From the analyses in Sect. 3, it can be concluded that it is mudcake thickness and permeability, rather than mudcake strength, which modify wellbore stress and FIP. Thicker and tighter mudcakes can better enhance FIP. The main mechanism for FIP enhancement is related to wellbore pressure diffusion. The wellbore pressure is free to diffuse into the surrounding formation when there is no mudcake on the wellbore wall (Figs. 2, 6). The small true overbalance pressure (i.e., the difference between wellbore pressure and pore pressure close to the wellbore) in this case results in lower FIP. On the other hand, when a mudcake exists, the true overbalance pressure and consequently FIP can be significantly increased (Figs. 2, 6). A quality mudcake for preventing near-wellbore pressure diffusion can be obtained by adding proper additives to the mud. Generally, standard filtration additives can satisfy the need for sandstone formations. However, for shale with low pore size ($\sim$ 0.01 micron) and permeability ($\sim$ 0.01 mD or less), specially engineered mud additives are required for forming a tight mudcake (Ewy and Morton 2009). Mud formulations are beyond the scope of this paper, and readers are referred to Ewy and Morton (2009) for tests of four different commercial muds on preventing pore pressure diffusion in shales.

The model proposed in this paper can be used to predict FIP with the presence of a mudcake on the wellbore. However, it is necessary to distinguish FIP from FLP. Fluid loss occurs only after a fracture has been created and the wellbore fluid is flowing into the fracture. For a wellbore without mudcake, FIP should be equal to FLP because once a fracture initiates the fluid will immediately enter and drive the extension of the fracture. However, when a mudcake exists, the fluid does not necessarily flow into the fracture when a fracture occurs on the wellbore wall. This phenomenon can be caused by two mechanisms as follows.

First, the micro-fracture induced by FIP can be quickly sealed by the mudcake because of the good flow capability of the plastic mudcake, as shown in Fig. 14. The 'internal' mudcake in the fracture can then isolate the fracture tip from wellbore pressure. Hence, a wellbore pressure higher than FIP is required to break this 'internal' mudcake for fracture extension and fluid flow into the fracture.

A second mechanism has been identified. Even though the small fracture induced by FIP is not fully sealed, the mudcake on the wellbore wall does not necessary break. Rather, the mudcake can still bridge over the fracture opening at the fracture mouth as shown in Fig. 15a. In other words, the narrow fracture can initiate and propagate to some extent behind the mudcake without disrupting it (Cook et al. 2016). Under such conditions, the mudcake still prevents fluid flow into the fracture. Growth of the fracture is not driven by the fluid pressure acting on the fracture surface, but rather by the wellbore pressure exerted on the wellbore wall. Only with continuous increase in wellbore pressure, will the mudcake across the fracture opening be broken, allowing fluid to enter the fracture and cause rapid fracture growth. Therefore, FLP could be significantly higher than FIP. This conclusion has been confirmed by a series of laboratory wellbore strengthening tests by Guo et al. (2014). In the tests, the fractures were found to extend a long distance, even completely through the rock specimens, without indication of fluid loss. This observation implies that FLP must be larger than FIP due to the bridging/sealing effect of the mudcake.

The rupture of the mudcake over the fracture mouth may have two distinguishing failure modes (Cook et al. 2016): (1) tensile failure—the mudcake is pulled apart by the opening fracture as shown in Fig. 15b, and (2) shear failure—the mudcake is pushed into the fracture by wellbore pressure as shown in Fig. 15c. For these two failure modes, the mudcake strength is an important factor controlling the critical wellbore pressure for mudcake rupture and thus

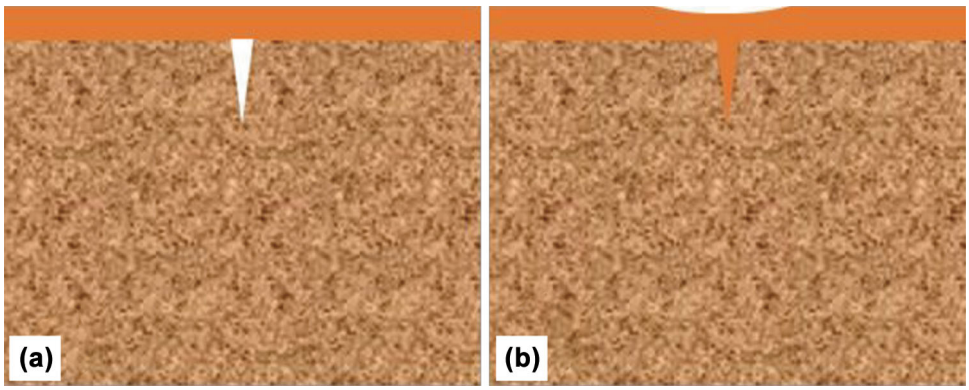

Fig. 14 Schematic of 'internal' mudcake in the fracture. **a** A micro-fracture (white) created at FIP. **b** The micro-fracture is filled with mudcake (orange)

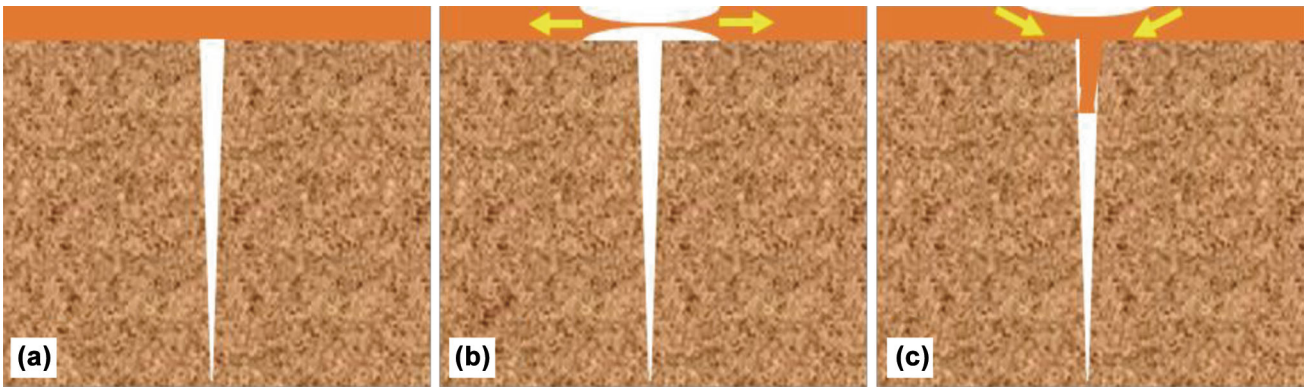

Fig. 15 Schematic of mudcake bridge (orange) over the fracture (white) mouth and its failure mechanisms. **a** A mudcake bridges over the mouth of a fracture. **b** Tensile failure of the mudcake. **c** Shear failure of the mudcake. Modified after Cook et al. (2016)

FLP, although it has a small influence on FIP. The mudcake strength is a function of mud type, particle size, particle strength, etc. Aadnøy and Belayneh (2004) have experimentally shown that particles with higher strength can form a stronger mudcake bridge over the fracture mouth. Cook et al. (2016) have indicated that a mudcake formed from oil-based mud is much weaker that of the water-based mud because the lubricating emulsion droplets in the oil-based mud reduce the particle–particle strength in the mudcake. For more detailed information on the effect of mudcake strength on wellbore strengthening, the readers are referred to Cook et al. (2016) and Aadnoy and Belayneh (2004).

6 Conclusions

An analytical model for predicting near-wellbore stress distribution and wellbore FIP considering the effects of mudcake has been derived in this paper. Numerical examples have been provided to illustrate the effects of mudcake thickness, permeability and strength on wellbore stress and FIP. The implications of the analysis on wellbore strengthening have been discussed. The following conclusions are drawn from the studies in this paper.

(1) The presence of a mudcake on the wellbore wall can effectively prevent the development of tensile stresses around the wellbore and consequently maintain a relatively large FIP.
(2) A mudcake enhances wellbore stress and FIP mainly through restricting pore pressure increase in the near-wellbore region, rather than by the mudcake strength.
(3) A thicker and tighter mudcake can improve wellbore strengthening effect. But a thicker mudcake can cause differential sticking, excessive torque and drag, etc.
(4) Even with a very thin mudcake (e.g., 2 mm), FIP can be effectively elevated compared with the case without mudcake on the wellbore.
(5) Despite very low permeability of the mudcake (e.g., 10^{-3} mD), neglecting the permeable nature of the

mudcake, i.e., assuming the mudcake is impermeable, may lead to substantial overestimation of FIP.

(6) FLP is different from FIP when a mudcake exists on the wellbore wall. Fractures may occur behind the mudcake without mudcake rupture. FLP is usually greater than FIP because a higher wellbore pressure is required to break the mudcake sealant in the fracture or the mudcake bridge over the fracture opening at the fracture mouth.

(7) The small effect of mudcake strength on FIP does not mean its effect on FLP is also small. Mudcake strength plays an important role in maintaining mudcake integrity and thus the wellbore pressure once a fracture has initiated behind the mudcake.

(8) In general, an optimal mudcake for wellbore strengthening applications should have a moderate thickness, low permeability, and high strength. Proper design of mud formulations according to the drilling and formation conditions is important for achieving a quality mudcake.

Acknowledgements The authors wish to thank the Wider Windows Industrial Affiliate Program, the University of Texas at Austin, for financial and logistical support of this work. Program support from BHP Billiton, British Petroleum, Chevron, ConocoPhillips, Halliburton, Marathon, National Oilwell Varco, Occidental Oil and Gas, and Shell is gratefully acknowledged.

References

Aadnøy BS, Belayneh M. Elasto-plastic fracturing model for wellbore stability using non-penetrating fluids. J Pet Sci Eng. 2004;45:179–92. https://doi.org/10.1016/j.petrol.2004.07.006.

Alberty MW, McLean MR. A physical model for stress cages. In: SPE annual technical conference and exhibition, 26–29 Sept, Houston; 2004. https://doi.org/10.2118/90493-MS.

Amanullah M, Tan CP. January. A non-destructive method of cake thickness measurement. In: SPE Asia Pacific oil and gas conference and exhibition. 16–18 Oct, Brisbane; 2000. https://doi.org/10.2118/64517-MS.

Amanullah M, Tan CP. A field applicable laser-based apparatus for mudcake thickness measurement. In: SPE Asia Pacific oil and gas conference and exhibition, 17–19 Apr, Jakarta; 2001. https://doi.org/10.2118/68673-MS.

Arlanoglu C, Feng Y, Podnos E, Becker E, Gray KE. Finite element studies of wellbore strengthening. In: IADC/SPE drilling conference and exhibition, 4–6 March, Fort Worth; 2014. https://doi.org/10.2118/168001-MS.

Aston MS, Alberty MW, Duncum SD, Bruton JR, Friedheim JE, Sanders MW. A new treatment for wellbore strengthening in shale. In: SPE annual technical conference and exhibition, 11–14 Nov, Anaheim; 2007. https://doi.org/10.2118/110713-MS.

Badrul MJ, Chiou LL, Azlina Z, Juliana Z. Dolomite as an alternative weighting agent in drilling fluids. J Eng Sci Technol. 2007;2(2):164–76.

Bageri BS, Al-Mutairi SH, Mahmoud M. Different techniques for characterizing the filter cake. In: SPE unconventional gas conference and exhibition. 28–30 Jan, Muscat; 2013. https://doi.org/10.2118/163960-MS.

Bailey L, Meeten G, Way P, L'alloret F. Filtercake integrity and reservoir damage. In: SPE formation damage control conference, 18–19 Feb, Lafayette; 1998. https://doi.org/10.2118/39429-MS.

Berntsen AN, Robbes AS, Cerasi PR, Van Der Zwaag CH. Laboratory investigation of brine diffusion through oil-based mud filter cakes. In: SPE international symposium and exhibiton on formation damage control, 10–12 Feb, Lafayette; 2010. https://doi.org/10.2118/128027-MS.

Bezemer C, Havenaar I. Filtration behavior of circulating drilling fluids. SPE J. 1966;6:292–8. https://doi.org/10.2118/1263-PA.

Cerasi P, Ladva HK, Bradbury AJ, Soga K. Measurement of the mechanical properties of filtercakes. In: SPE European formation damage conference, 21–22 May, The Hague; 2001. https://doi.org/10.2118/68948-MS.

Chenevert ME, Dewan JT. A model for filtration of water-base mud during drilling: determination of mudcake parameters. Petrophysics. 2001;42(3):237–50.

Chuanliang Y, Jingen D, Xiangdong L, Xiaorong L, Yongcun F. Borehole stability analysis in deepwater shallow sediments. J Energy Res Technol. 2015;137(1):012901. https://doi.org/10.1115/1.4027564.

Cook J, Guo Q, Way P, Bailey L, Friedheim J. The role of filtercake in wellbore strengthening. In: IADC/SPE drilling conference and exhibition, 1–3 March, Fort Worth; 2016. https://doi.org/10.2118/178799-MS.

Cui L, Abousleiman Y, Cheng AH, Roegiers JC. Time-dependent failure analysis of inclined boreholes in fluid-saturated formations. J Energy Res Technol. 1999;121(1):31–9. https://doi.org/10.1115/1.2795057.

Cui L, Cheng AH, Abousleiman Y. Poroelastic solution for an inclined borehole. J Appl Mech. 1997;64(1):32–8. https://doi.org/10.1115/1.2787291.

Dangou MA, Chandler H. Potential increase of formation damage at horizontal wells as a result of changing dynamic filter cake parameters with the shear rate. In: The 8th European formation damage conference, 27–29 May, Scheveningen; 2009. https://doi.org/10.2118/120867-MS.

Ewy RT, Morton EK. Wellbore-stability performance of water-based mud additives. SPE Drill Complet. 2009;24:390–7. https://doi.org/10.2118/116139-PA.

Feng Y, Arlanoglu C, Podnos E, Becker E, Gray KE. Finite-element studies of hoop-stress enhancement for wellbore strengthening. SPE Drill Complet. 2015;30:38–51. https://doi.org/10.2118/168001-PA.

Feng Y, Gray KE. A parametric study for wellbore strengthening. J Nat Gas Sci Eng. 2016a;30:350–63. https://doi.org/10.1016/j.jngse.2016.02.045.

Feng Y, Gray KE. A fracture-mechanics-based model for wellbore strengthening applications. J Nat Gas Sci Eng. 2016b;29:392–400. https://doi.org/10.1016/j.jngse.2016.01.028.

Feng Y, Jones JF, Gray KE. A review on fracture-initiation and -propagation pressures for lost circulation and wellbore strengthening. SPE Drill Complet. 2016;31:134–44. https://doi.org/10.2118/181747-PA.

Feng Y, Li X, Gray KE. An easy-to-implement numerical method for quantifying time-dependent mudcake effects on near-wellbore

stresses. J Pet Sci Eng. 2018. https://doi.org/10.1016/j.petrol.2018.01.051.
Fjar E, Holt RM, Raaen AM, Risnes R, Horsrud P. Petroleum related rock mechanics. Amsterdam: Elsevier; 2008.
Griffith J, Osisanya SO. Effect of drilling fluid filter cake thickness and permeability on cement slurry fluid loss. J Can Pet Technol. 1999. https://doi.org/10.2118/99-13-15.
Guo J, Luo B, Lu C, Lai J, Ren J. Numerical investigation of hydraulic fracture propagation in a layered reservoir using the cohesive zone method. Eng Fract Mech. 2017a;186:195–207. https://doi.org/10.1016/j.engfracmech.2017.10.013.
Guo Q, Cook J, Way P, Ji L, Friedheim JE. A comprehensive experimental study on wellbore strengthening. In: IADC/SPE drilling conference and exhibition, 4–6 March, Fort Worth; 2014. https://doi.org/10.2118/167957-MS.
Guo T, Li Y, Ding Y, Qu Z, Gai N, Rui Z. Evaluation of acid fracturing treatments in shale formation. Energy Fuels. 2017b;31(10):10479–89. https://doi.org/10.1021/acs.energyfuels.7b01398.
Haberfield CM, Johnston IW. Relationship between fracture toughness and tensile strength for geomaterials. In: International conference on soil mechanics and foundation engineering, 12th, 1989, Rio de Janiero. 1989. pp. 47–52.
Haimson B, Fairhurst C. In-situ stress determination at great depth by means of hydraulic fracturing. In: The 11th U.S. symposium on rock mechanics (USRMS), American Rock Mechanics Association. 1969.
Hashemzadeh SM, Hajidavalloo E. Numerical investigation of filter cake formation during concentric/eccentric drilling. J Pet Sci Eng. 2016;145:161–7. https://doi.org/10.1016/j.petrol.2016.03.024.
Hubbert MK, Willis DG. Mechanics of hydraulic fracturing. SPE-686-G. Richardson: SPE; 1957. p. 153–68.
Jaffal HA, El Mohtar CS, Gray KE. Modeling of filtration and mudcake buildup: an experimental investigation. J Nat Gas Sci Eng. 2017;38:1–11. https://doi.org/10.1016/j.jngse.2016.12.013.
Khan K, Al-Shayea NA. Effect of specimen geometry and testing method on mixed mode I–II fracture toughness of a limestone rock from Saudi Arabia. Rock Mech Rock Eng. 2000;33:179–206. https://doi.org/10.1007/s006030070006.
Lee D, Bratton T, Birchwood R. Leak-off test interpretation and modeling with application to geomechanics. In: Gulf Rocks 2004, the 6th North America Rock mechanics symposium (NARMS). American Rock Mechanics Association. 2004.
Liu X, Civan F. Formation damage and skin factor due to filter cake formation and fines migration in the near-wellbore region. In: SPE formation damage control symposium, 7–10 Feb, Lafayette; 1994. https://doi.org/10.2118/27364-MS.
Meeten GH, Sherwood JD. Vane technique for shear-sensitive and wall-slipping fluids. In: Moldenaers P, Keunings R, editors. Theoretical and applied rheology. Richardson: Society of Petroleum Engineers; 1992. p. 935–7.
Morita N, Fuh GF. Parametric analysis of wellbore-strengthening methods from basic rock mechanics. SPE Drill Complet. 2012;27:315–27. https://doi.org/10.2118/145765-PA.
Mostafavi V, Hareland G, Aadnøy BS, Kustamsi A. Modeling of fracture and collapse initiation gradients in presence of mud cake. In: ISRM international symposium—EUROCK 2010, 5–18 June, Lausanne; 2010. ISRM-EUROCK-2010-168.
OttesenS, Benaissa S, Marti J. Down-hole simulation cell for measurement of lubricity and differential pressure sticking. In: SPE/IADC drilling conference, 9–11 March, Amsterdam; 1999. https://doi.org/10.2118/52816-MS.
Outmans HD. Mechanics of differential pressure sticking of drill collars. Richardson: Society of Petroleum Engineers; 1958.
Rui Z, Lu J, Zhang Z, Guo R, Ling K, Zhang R, et al. A quantitative oil and gas reservoir evaluation system for development. J Nat Gas Sci Eng. 2017a;42:31–9. https://doi.org/10.1016/j.jngse.2017.02.026.
Rui Z, Li C, Peng F, Ling K, Chen G, Zhou X, et al. Development of industry performance metrics for offshore oil and gas project. J Nat Gas Sci Eng. 2017b;39:44–53. https://doi.org/10.1016/j.jngse.2017.01.022.
Rui Z, Peng F, Ling K, Chang H, Chen G, Zhou X. Investigation into the performance of oil and gas projects. J Nat Gas Sci Eng. 2017c;38:12–20. https://doi.org/10.1016/j.jngse.2016.11.049.
Rui Z, Wang X, Zhang Z, Lu J, Chen G, Zhou X, et al. A realistic and integrated model for evaluating oil sands development with steam assisted gravity drainage technology in Canada. Appl Energy. 2018;213:76–91. https://doi.org/10.1016/j.apenergy.2018.01.015.
Salehi S, Kiran R. Integrated experimental and analytical wellbore strengthening solutions by mud plastering effects. J Energy Resour Technol. 2016;138:032904–7. https://doi.org/10.1115/1.4032236.
Sepehrnoori K, Proett MA, Wu J, Torres-Verd¡n C. The influence of water-base mud properties and petrophysical parameters on mudcake growth, filtrate invasion, and formation pressure. Petrophysics. 2005;46(1):14–32.
Sherwood JD, Meeten GH, Farrow CA, Alderman NJ. Squeeze-film rheometry of non-uniform mudcakes. J Nonnewton Fluid Mech. 1991;39(3):311–34. https://doi.org/10.1016/0377-0257(91)80020-K.
Song J, Rojas JC. Preventing mud losses by wellbore strengthening. In: SPE Russian oil and gas technical conference and exhibition, 3–6 Oct, Moscow; 2006. https://doi.org/10.2118/101593-MS. https://doi.org/10.2118/101593-ms.
Tran M, Abousleiman Y, Nguyen V. The effects of filter-cake buildup and time-dependent properties on the stability of inclined wellbores. SPE J. 2011;16(4):1010–28. https://doi.org/10.2118/135893-PA.
Wang H, Soliman MY, Towler BF. Investigation of factors for strengthening a wellbore by propping fractures. SPE Drill Complet. 2009;24:441–51. https://doi.org/10.2118/112629-PA.
Whittaker BN, Singh RN, Sun G. Rock fracture mechanics: principles, design, and applications. Amsterdam: Elsevier; 1992.
Zhang ZX. An empirical relation between mode I fracture toughness and the tensile strength of rock. Int J Rock Mech Min Sci. 2002;39:401–6. https://doi.org/10.1016/S1365-1609(02)00032-1.
Zhang ZX, Kou SQ, Lindqvist PA, Yu Y. The relationship between the fracture toughness and tensile strength of rock. In: Yu M-H, editor. Strength theories: applications, development & prospects for 21st century. Beijing/NewYork: Science Press; 1998. p. 215–9.
Zhao P, Santana CL, Feng Y, Gray KE. Mitigating lost circulation: a numerical assessment of wellbore strengthening. J Pet Sci Eng. 2017;157:657–70. https://doi.org/10.1016/j.petrol.2017.07.052.
Zhu H, Guo J, Zhao X, Lu Q, Luo B, Feng Y. Hydraulic fracture initiation pressure of anisotropic shale gas reservoirs. Geomech Eng. 2014;7:403–30.
Ziegler FE, Jones JF. Predrill pore-pressure prediction and pore pressure and fluid loss monitoring during drilling: a case study for a deepwater subsalt Gulf of Mexico well and discussion on fracture gradient, fluid losses, and wellbore breathing. Interpretation. 2014;2:SB45–55. https://doi.org/10.1190/INT-2013-0099.1.
Zoback MD. Reservoir geomechanics. Cambridge: Cambridge University Press; 2010.